Reprinted from "Polarization: Measurement, Analysis, and Remote Sensing," D. H. Goldstein and Russell A. Chipman, Editors, Proc. SPIE 3121, 173-182 (1997)

Bidirectional ellipsometry and its application to the characterization of surfaces

Thomas A. Germer and Clara C. Asmail

Optical Technology Division
National Institute of Standards and Technology
Gaithersburg, Maryland 20899

ABSTRACT

The polarization of light scattered out of the plane of incidence was measured from rough and microrough silicon, polished fused silica and glass ceramic, and ground and polished black glass. The measurement results are in excellent agreement with models for scattering from microroughness or subsurface defects, demonstrating that the polarization of scattered light can be used to distinguish between microroughness and subsurface defects.

Keywords: polarimetry, scatter, surfaces, microroughness, subsurface defects

1. INTRODUCTION

The amount of light scattered by a material is often a sensitive measure of the quality of that material.[1] Since a perfectly smooth surface of a material having translational symmetry will not scatter light, any defects, be it roughness, subsurface defects, grain structure, or particulate contamination, will scatter light into directions away from the specular or transmitted directions. It is therefore common to measure the bidirectional reflectance distribution function (BRDF), the fraction of incident light scattered per unit projected solid angle, or a solid-angle-integrated BRDF, to assess the condition of materials such as bare silicon wafers, magnetic and optical storage media, mirrors, flat panel displays or other optical quality materials.[2,3] Although different characteristic defects on any particular material sometimes have signature BRDFs that allow them to be distinguished, in general the BRDF lacks the capability of distinguishing between the different sources of scatter.

On the other hand, the polarization of the light can indicate the path that the light followed during its trajectory. For example, light scattered by a particle above the surface of the material undergoes different trajectories than light which is scattered by the roughness of the surface or by a defect below the surface. This effect is expected to be most pronounced for scattering of obliquely incident light into directions out of the plane of incidence, since these directions allow the viewing instrument to best observe the rotations of the electric field that occur upon refraction and reflection. Therefore, the polarization of out-of-plane scattered light should strongly track the sources of that scattered light.

Although polarized light scattering has been prevalent in studies of scattering in particles,[4,5] its use has been limited in the study of surfaces.[6–10] Much of this disuse has been a combined result of instrumentation issues and the interpretation of the results. From the instrumentation side, measurements of light scattered out of the plane of incidence add extra degrees of freedom that are not present in the measurements of free particle scattering. On the interpretation side, few models have guided the experimentalist to the quickest and most efficient measurement. For example, the elements of the Mueller matrix BRDF, the polarimetric generalization of the BRDF, do not neccesarily map directly onto those properties of the material which are relevant to understanding the origin of the scattered light. That is, one cannot simply take a particular element of the Mueller matrix BRDF and assign its magnitude to the density of a particular type of defect.

It is shown in this paper that a less generalized polarimetric treatment of the scattered light, bidirectional ellipsometry,[11] contains some powerful properties that allow it to determine the location of scattering centers. In bidirectional ellipsometry, light with a particular linear polarization state is incident onto the surface, and the direction of the polarization of the scattered light is mapped out with a detection polarizer, yielding an angle of

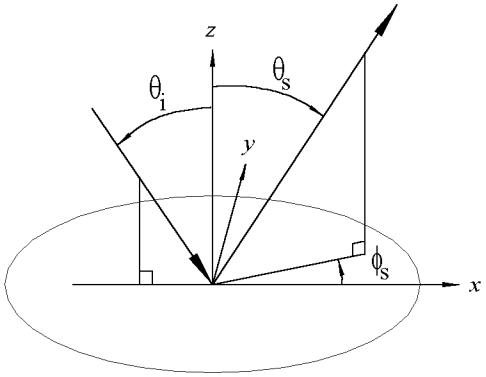

Figure 1 The sample coordinate system.

scattered polarization and a degree of linear polarization. It is shown that the angle of scattered polarization is a sensitive measure of the origin of the scattered light.

In Section II, simple model predictions for scattering from subsurface spheres and microroughness will be reviewed. The experiment by which these models will be tested will be outlined in Sec. III. The results of these measurements will be presented in Sec. IV. Section V will discuss these results, comparing them to the model predictions. Finally, the conclusions of the paper will be set forth in Sec. VI.

2. THEORY

Theories for scattering from particulate contaminants and subsurface defects in the Rayleigh limit and from microtopography have been developed elsewhere.[12] In this section, we summarize the results of the subsurface defect and microroughness theories. Each of these theories predicts the form of the Jones scattering matrix,

$$\begin{pmatrix} ss & ps \\ sp & pp \end{pmatrix}$$

which relates the scattered electric field to the incident electric field. Overall factors which are common to all four elements of the matrix do not affect the polarization of the light and will not be discussed in this paper. The basis set used to describe the polarization will be $\{\hat{\mathbf{s}}, \hat{\mathbf{p}}, \hat{\mathbf{k}}\}$, where $\hat{\mathbf{k}}$ is a unit vector in the direction of propagation, $\hat{\mathbf{s}}$ is a unit vector perpendicular to the plane of incidence (or viewing), and $\hat{\mathbf{p}} = \hat{\mathbf{k}} \times \hat{\mathbf{s}}$ is a unit vector in the plane of incidence (or viewing). The substrate material is assumed to have a dielectric constant ϵ at the wavelength of the incident light, λ. The coordinate system used to describe the incident and scattered light directions is outlined in Fig. 1. The z axis coincides with the surface normal, and light is assumed to be incident at an angle θ_i in the x-z plane. The direction of scattered light is parameterized by its polar angle θ_s and azimuthal angle ϕ_s.

Spheres small enough to be considered in the Rayleigh limit located below a surface will lead to a Jones scattering matrix given by

$$\begin{pmatrix} k\cos\phi_\mathrm{s}/[(k_{z\mathrm{i}}+k'_{z\mathrm{i}})(k_{z\mathrm{s}}+k'_{z\mathrm{s}})] & -k'_{z\mathrm{i}}\sin\phi_\mathrm{s}/[(\epsilon k_{z\mathrm{i}}+k'_{z\mathrm{i}})(k_{z\mathrm{s}}+k'_{z\mathrm{s}})] \\ -k'_{z\mathrm{s}}\sin\phi_\mathrm{s}/[(k_{z\mathrm{i}}+k'_{z\mathrm{i}})(\epsilon k_{z\mathrm{s}}+k'_{z\mathrm{s}})] & (k_{xy\mathrm{i}}k_{xy\mathrm{s}}-k'_{z\mathrm{i}}k'_{z\mathrm{s}}\cos\phi_\mathrm{s})/[(\epsilon k_{z\mathrm{i}}+k'_{z\mathrm{i}})(\epsilon k_{z\mathrm{s}}+k'_{z\mathrm{s}})] \end{pmatrix}, \tag{1}$$

where

$$k_{zj} = k\cos\theta_j,$$

$$k_{xyj} = k\sin\theta_j,$$

$$k'_{zj} = k\sqrt{\epsilon - \sin^2\theta_j},$$

$k = 2\pi/\lambda$ is the magnitude of the vacuum wavevector, and j is either s or i. This model accounts for refraction at the interface and the transmission coefficients. The correlations between defects, the penetration of the light into the material, the escape of the scattered light out of the material, the characteristic optical constant and size of the defect, and the wavelength of the light, λ, do not effect the polarization, but rather contribute to terms common to all four Jones matrix elements.

In the smooth surface limit, where first-order vector perturbation theory (Rayleigh-Rice theory) can be applied, the scattering from microroughness has a characteristic Jones matrix given by

$$\begin{pmatrix} k\cos\phi_{\rm s}/[(k_{z{\rm i}}+k'_{z{\rm i}})(k_{z{\rm s}}+k'_{z{\rm s}})] & -k'_{z{\rm i}}\sin\phi_{\rm s}/[(\epsilon k_{z{\rm i}}+k'_{z{\rm i}})(k_{z{\rm s}}+k'_{z{\rm s}})] \\ -k'_{z{\rm s}}\sin\phi_{\rm s}/[(k_{z{\rm i}}+k'_{z{\rm i}})(\epsilon k_{z{\rm s}}+k'_{z{\rm s}})] & (\epsilon k_{xy{\rm i}}k_{xy{\rm s}}-k'_{z{\rm i}}k'_{z{\rm s}}\cos\phi_{\rm s})/[(\epsilon k_{z{\rm i}}+k'_{z{\rm i}})(\epsilon k_{z{\rm s}}+k'_{z{\rm s}})] \end{pmatrix}. \tag{2}$$

Again, the surface height correlation function and the optical wavelength contribute only to terms common to all four elements, and therefore do not effect the polarization.

It can be seen from Eqs. (1) and (2) that the ss, ps, and sp Jones matrix elements for the two mechanisms are identical, and that the pp elements differ, and then only if the $\theta_{\rm i}$ and $\theta_{\rm s}$ are nonzero. To exploit the polarization of scattered light to distinguish between these two mechanisms, it is neccesary that some p-polarized light be involved in both the incident and scattered light, that there be some contribution from at least one of the ss, ps, and sp Jones matrix elements, that the light be incident at an oblique angle, and that the viewing angle be oblique. Comparison of the pp elements suggests that further contrast between the two mechanisms can be achieved if $\phi_{\rm s}$ is varied; that is, one views the sample out of the plane of incidence. This contrast is then maximized by using either purely p-polarized incident light or p-polarized viewing light.

The conditions outlined above allowing a distinction between the two mechanisms by bidirectional ellipsometry are also met for in-plane measurements with light incident with a combination of s and p polarizations, e.g. 45° polarized light. However, this practice relies on interference between the pp element and the three other elements, whereas the practice of measuring the polarization of out-of-plane scattered light for p-polarized incident light (or visa versa) relies only on interference between the pp element and one other element. For this reason, it is expected that the polarization of out-of-plane scattered light for p-polarized incident light will be more sensitive to the scattering mechanism.

3. EXPERIMENT

The Goniometric Optical Scatter Instrument (GOSI) which was used to perform the measurements described in this paper is described elsewhere.[13,14] Briefly, the second harmonic of a Nd:YAG laser ($\lambda = 532$ nm) is incident onto a sample at an angle $\theta_{\rm i}$, and light scattered into the direction defined by the angles $\{\theta_{\rm s}, \phi_{\rm s}\}$ is collected. The polarization state of the incident light is selected with a fixed linear polarizer followed by a rotatable $\lambda/2$ linear retarder. The polarization state of the scattered light is analyzed with a rotatable $\lambda/2$ linear retarder followed by a fixed linear polarizer. Although a bidirectional ellipsometric measurement can be carried out by fixing the incident light polarization while rotating the detection polarization optics, all of the measurements described in this paper were made by measuring the 3×3 non-handed Mueller matrix using a $(\omega, 4\omega)$ scheme,[15] whereby the receiving retarder is rotated at four times the rate of the incident light retarder. The signal is measured at 16 evenly spaced intervals, and the 9 elements of the 3×3 non-handed Mueller matrix are determined from the Fourier transform of those signals.

The angle η that the principle axis of the polarization ellipse makes with respect to the $\hat{\mathbf{s}}$ axis when the incident light is p-polarized can then be determined from the Mueller matrix to be[16]

$$\eta = \frac{1}{2}\arctan(M_{21} - M_{22}, M_{31} - M_{32}), \tag{3}$$

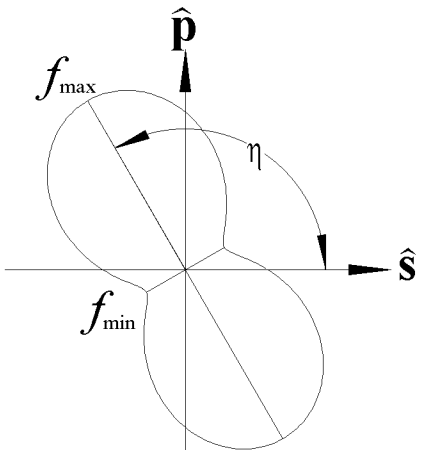

Figure 2 A schematic of the intensity distribution measured by a rotating linear polarizer, defining the angle η and the maximum and minimum signals, $f_{\max}$ and $f_{\min}$, respectively. The axes are defined so that the viewer is looking into the scattered beam.

where the two-argument arctangent is given by

$$\arctan(x,y) = \left\{ \begin{array}{cc} \arctan(y/x) & \text{if } x > 0 \\ \pi + \arctan(-y/x) & \text{if } x < 0 \\ \pi/2 & \text{if } x = 0 \text{ and } y > 0 \\ -\pi/2 & \text{if } x = 0 \text{ and } y < 0 \end{array} \right\}. \tag{4}$$

As a measure of the degree to which the light is linearly polarized, the degree of linear polarization is

$$\text{DOLP} = \frac{f_{\max} - f_{\min}}{f_{\max} + f_{\min}} = \frac{\sqrt{(M_{21} - M_{22})^2 + (M_{31} - M_{32})^2}}{M_{11} - M_{12}}, \tag{5}$$

where $f_{\max}$ and $f_{\min}$ are the maximum and minimum scattered light signals as an analyzing linear polarizer is rotated, respectively (see Fig. 2). For linearly polarized light, DOLP = 1, and for purely depolarized light or completely circularly polarized light, DOLP = 0.

By focussing attention on the principle axis of the polarization ellipse, certain issues can be ignored. Foremost of these is the scattering from other objects in the room which are illuminated by the specular beam. This light is most likely to be highly depolarized, and therefore will have little effect on the measurement of η.

For all of the measurements reported in this paper, the incident angle was $\theta_{\text{i}} = 45°$ and the polar scattering angle was $\theta_{\text{s}} = 45°$. The azimuthal scattering angle ϕ_{s} was varied so that the polarization of scattered light into a cone was mapped out, and all but the extremes of the domain correspond to scattering out of the plane of incidence.

The polarization of optical scattering from a variety of samples was measured, each chosen for its capability of demonstrating the theories above. Three silicon samples were measured, two which were photolithographically (SiA and SiB) designed to exhibit surface microroughness of two different levels,[17] and the third was the rough backside of a silicon wafer (SiC). The BRDF levels of these silicon samples in the 0°/45° incident/viewing configuration were approximately 10^{-6} sr^{-1}, 10^{-4} sr^{-1}, and 10^{-2} sr^{-1}, respectively.

Two additional samples were used to test the model for subsurface defects. The first (FS) was a highly polished piece of high grade fused silica. Due its polycrystaline structure, fused silica exhibits a small degree of bulk Rayleigh scatter. The scattering extinction coefficient was measured to be about 2×10^{-5} cm^{-1} (base e). At angles close to the specular direction the scattered light is expected to be dominated by surface figure, while at

larger angles, the total scatter is dominated by the scatter from the bulk. The second of these samples (ZD) was a polished piece of glass ceramic (Zerodur[18]), a material whose scattering extinction coefficient was measured to be about 7×10^{-2} cm^{-1} (base e).

The full power of bidirectional ellipsometry is its ability to distinguish between different scattering mechanisms. A series of Schott[18] UG1 visible light absorbing glass samples[19] was chosen, each ground and polished to different degrees so as to exhibit a variety of BRDF levels. These samples are expected to exhibit a combination of microroughness and subsurface damage. These samples (BgA, BgB, BgC, BgD, BgE, and BgF) exhibited BRDF levels in the 0°/45° incident/viewing configurations of approximately 7×10^{-6} sr^{-1}, 3×10^{-5} sr^{-1}, 2×10^{-3} sr^{-1}, 7×10^{-3} sr^{-1}, 9×10^{-3} sr^{-1}, and 1×10^{-2} sr^{-1}, respectively.

The random and systematic measurement uncertainties for η and DOLP can be estimated by performing a series of measurements of these values with the receiver in the path of the incident light and without the presence of a sample. A series of eighty measurements yielded values of $\eta = 90.08°$ and DOLP $= 0.9993$. These values differ from the theoretical values of $\eta = 90°$ and DOLP $= 1$ due to systematic errors. The standard deviations, $\sigma_\eta = 0.01°$ and $\sigma_{\mathrm{DOLP}} = 0.0003$, represent the respective random uncertainties for a single measurement. Other random and systematic errors may contribute to uncertainties in the presence of a sample. Although a complete discussion of these uncertainties is beyond the scope of this paper, the expanded uncertainties (with a coverage factor of $k = 2$) of η and DOLP are not expected to exceed 5°and 0.05, respectively.

4. RESULTS AND DISCUSSION

Figures 3–5 show the results of bidirectional ellipsometric measurements on all of the samples. For each set of samples, we show the ellipsometric angle η and the degree of linear polarization, DOLP. The prediction of each theory, using Eqs. (1) and (2), is shown with each set of data. Both of the theories predict DOLP ~ 1; therefore, the results of the model DOLP are not shown.

There are two striking features that can be observed from the results shown in Figs. 3–5. First, the agreement between the measured polarization angles η and those predicted by theory is excellent. This feature suggests that different scattering mechanisms can indeed be distinguished by the polarization of the scattered light.

The second feature is the degree to which the light is linearly polarized. Although at large scattering angles, DOLP deviates from unity, the excellent agreement between theory and experiment for η suggests that the increasing depolarization is occuring because of the growing contribution of minority scattering mechanisms. For example, microrough surfaces might be expected to yield a small degree of subsurface features. Furthermore, nearly all surfaces include some oxide layer, which may modify the scattering characteristics to some degree. For the low scatter silicon samples (SiA and SiB), some of the apparent depolarization may be due to background scatter resulting from the specular beam striking the diffusely reflecting walls of the room.

The excellent agreement between the theory and experiment for microroughness, shown in Fig. 3, means that the polarization of light scattered by microroughness is not determined by the exact details of the surface height profile, but is a unique signature of the scattering mechanism. It therefore suggests that scatterometers can be designed to be blind to microroughness. For example, a device may be constructed with a number of detectors, each viewing a particular scattering direction, and each with a polarizer aligned to null the signal from microroughness.[20] Such a device would collect light over a large solid angle, be microroughness-blind, and therefore be more sensitive to other sources of scatter, such as subsurface defects and particulate contamination.

The rather low DOLP in the glass ceramic sample (ZD), shown in Fig. 4, is expected. The scattering extinction coefficient is very high so that multiple scattering will occur, the size of the grains is probably not small enough for Rayleigh scattering to be applicable, and those grains are not all of the same size and shape. The ability for bidirectional ellipsometry to extract a primary direction of polarization in such good agreement with the theory may at first glance be surprising, since the models for scattering from subsurface defects assume the

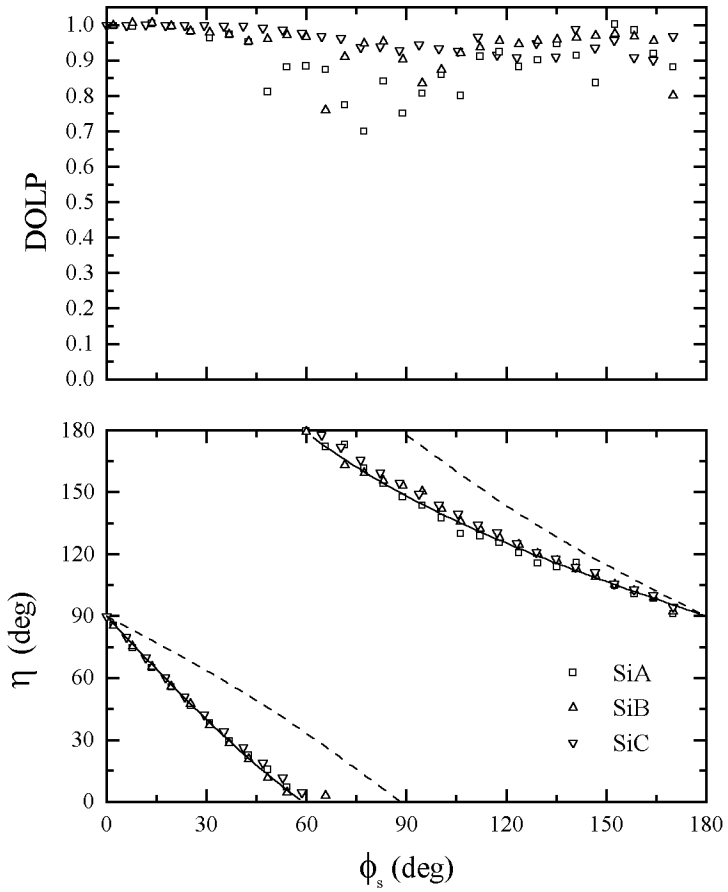

Figure 3 Results of bidirectional ellipsometry measurements for the three silicon samples (SiA, SiB, and SiC) as functions of the azimuthal scattering angle ϕ_s: (top) the degree of linear polarization (DOLP), and (bottom) the ellipsometric angle η. The incident and scattering polar angles were both 45°. The curves represent the models for surface microroughness (solid) and subsurface defects (dashed).

scatterers can be treated in the Rayleigh approximation. That is, the scattering centers are assumed to be point dipoles which polarize in the direction of the local electric field and locally radiate an electric field determined by $\mathbf{k} \times \mathbf{k} \times \mathbf{p}$, where $\mathbf{k}$ is the wavevector of the scattered light, and $\mathbf{p}$ is the dipole moment. However, simple symmetry arguments can be invoked to show that a random distribution of scattering centers will also polarize and radiate, on average, in the same manner. Therefore, when the scatterers are randomly oriented in the material, the primary direction of the polarization, η, is an indication of the local environment of the scatterers. Certainly, if all the defects within the illuminated region are aligned in a certain manner, and are not random, then there will be a preferential direction differing from that predicted by the Rayleigh approximation. Similarly, if a single non-Rayleigh scattering center is in the illuminated region, then the polarimetric behavior will reflect details of that scattering center, rather than that of an ensemble average.

The data for fused silica, shown in Fig. 4, agree very well with the subsurface model for out-of-plane scattering angles ϕ_s greater than $\sim 75°$. At these angles the scattered light is apparently dominated by the Rayleigh scattering in the material. For ϕ_s closer to the specular, however, the polarization of the scattered light deviates from the subsurface model and approaches the microroughness model. At these angles the scattered light is

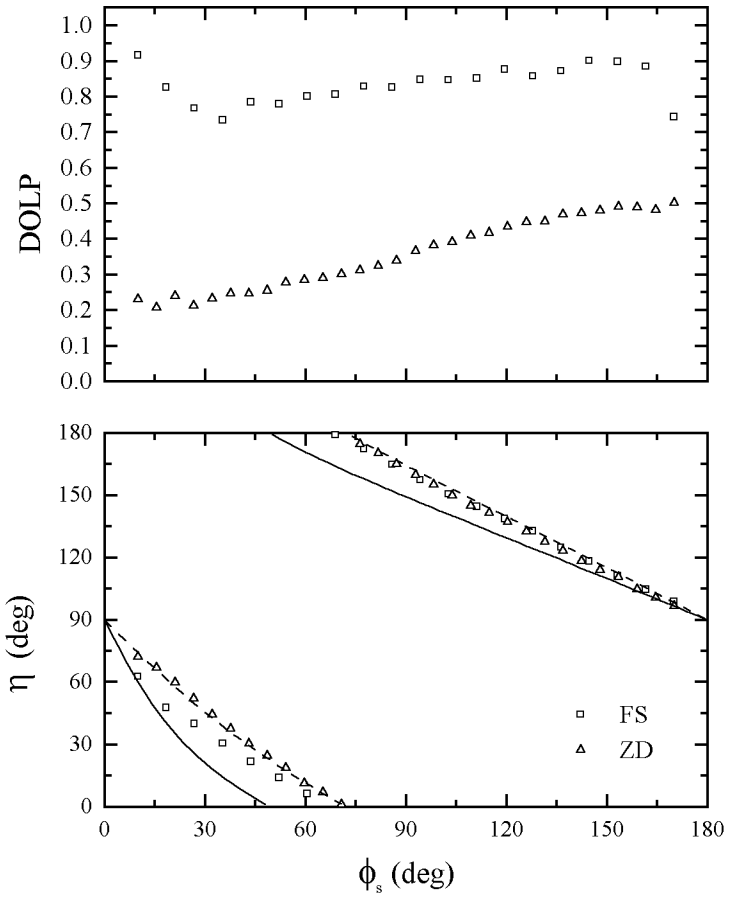

Figure 4 Results of bidirectional ellipsometry measurements for the two transparent samples (FS and ZD) as functions of the azimuthal scattering angle ϕ_s: (top) the degree of linear polarization (DOLP), and (bottom) the ellipsometric angle η. The incident and scattering polar angles were both 45°. The curves represent the models for surface microroughness (solid) and subsurface defects (dashed).

dominated by the surface finish of the sample. This behavior is not observed for the glass ceramic sample, since the subsurface scatter is over three orders of magnitude greater than that for fused silica. The fact that these two scattering sources can be distinguished in fused silica suggests that surface finish can be measured by polarized scattered light techniques, despite the existence of subsurface scatter.

Although the black glass data, shown in Fig. 5, appear to follow the microroughness model, they show a marked deviation toward the subsurface defect model, suggesting that both mechanisms are contributing to the scattered light, with a greater contribution arising from microroughness over most of the range of angles. This behavior is not surprising since some subsurface damage inevitably occurs during the polishing process. The ability for bidirectional ellipsometry to distinguish between the two mechanisms, and possibly assign a magnitude to the two contributions, suggests that the technique could prove useful in diagnosing manufacturing processes, where the types of defects that are created may be indicative of particular process deviations.

Models exist for scattering from particles on surfaces which predict the polarization of the scattered light to be different than that predicted for subsurface defects or microroughness. Although experimental results for

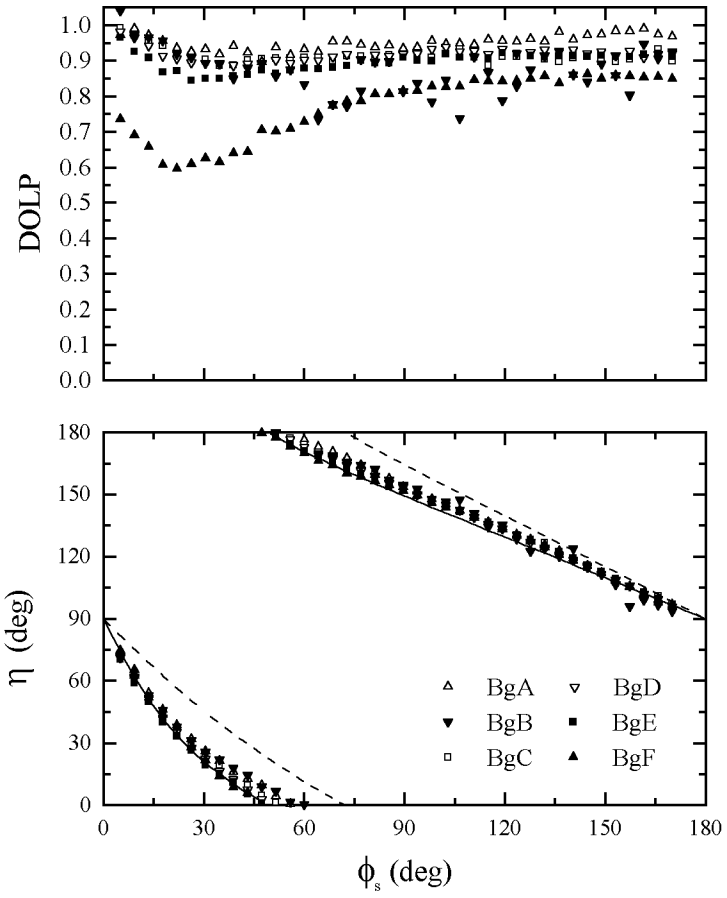

Figure 5 Results of bidirectional ellipsometry measurements for the six black glass samples (BgA, BgB, BgC, BgD, BgE, and BgF) as functions of the azimuthal scattering angle ϕ_s: (top) the degree of linear polarization (DOLP), and (bottom) the ellipsometric angle η. The incident and scattering polar angles were both 45°. The curves represent the models for surface microroughness (solid) and subsurface defects (dashed).

bidirectional ellipsometry measurements of particles on surfaces will be presented elsewhere, the technique of bidirectional ellipsometry should prove useful for distinguishing such particles from other sources of scatter such as microroughness. It is reasonable to speculate that bidirectional ellipsometry will be as applicable to the study of defects in thin films and roughness at thin film interfaces as specular ellipsometry is at characterizing thin films. The location of the source of scattering in a layered system, whether it be roughness in one of the interfaces, or disorder in one of the layers, should be discernible with bidirectional ellipsometry.

5. CONCLUSION

The results presented in this manuscript demonstrate that the primary polarization of scattered light from a variety of sources agrees very well with some simple models for optical scattering. Scattering from surface microroughness and subsurface features have characteristic polarimetric signatures that allow these two mechanisms to be distinguished.

ACKNOWLEDGEMENTS

The authors would like to thank Bradley Scheer of VLSI Standards, Inc. for supplying the microrough silicon samples, Robert Parks of the University of Arizona's Optical Sciences Center for manufacturing the black glass samples, and Mordechai Rothschild of MIT Lincoln Laboratory for supplying the fused silica sample.

REFERENCES

[1] J. C. Stover, *Optical Scattering: Measurement and Analysis*, (McGraw-Hill, New York, 1990).

[2] J. C. Stover, ed., *Optical Scattering in the Optics, Semiconductor, and Computer Disk Industries,* Proc. SPIE 2541 (1995).

[3] J. C. Stover, ed., *Flatness, Roughness, and Discrete Defect Characterization for Computer Disks, Wafers, and Flat Panel Displays,* Proc. SPIE 2862 (1996).

[4] C. F. Bohren, and D. R. Huffman, *Absorption and Scattering of Light by Small Particles*, (Wiley, New York, 1983).

[5] H. C. v. d. Hulst, *Light Scattering by Small Particles*, (Dover, New York, 1981).

[6] R. E. Luna, "Scattering by one-dimensional random rough metallic surfaces in a conical configuration: several polarizations," Opt. Lett. **21**, 1418–20 (1996).

[7] J. L. Pezzaniti, and R. A. Chipman, "Mueller matrix scatter polarimetry of a diamond-turned mirror," Opt. Eng. **34**, 1593–8 (1995).

[8] E. L. Church, and J. C. Stover, "Surface haze in the Stokes-Mueller representation," Proc. SPIE **2862**, 54–68 (1996).

[9] E. R. Méndez, A. G. Navarrete, and R. E. Luna, "Statistics of the polarization properties of one-dimensional randomly rough surfaces," J. Opt. Soc. Am. A **12**, 2507–16 (1995).

[10] S.-M. F. Nee, "Polarization of specular reflection and near-specular scattering by a rough surface," Appl. Opt. **35**, 3570–82 (1996).

[11] T. A. Germer, C. C. Asmail, and B. W. Scheer, "The polarization of out-of-plane scattering from microrough silicon," (submitted for publication.).

[12] T. A. Germer, "Angular dependence and polarization of out-of-plane optical scattering from particulate contamination, subsurface defects, and surface microroughness," (submitted for publication.).

[13] C. C. Asmail, C. L. Cromer, J. E. Proctor, and J. J. Hsia, "Instrumentation at the National Institute of Standards and Technology for bidirectional reflectance distribution function (BRDF) measurements," Proc. SPIE **2260**, 52–61 (1994).

[14] T. A. Germer, and C. C. Asmail, "A goniometric optical scatter instrument for bidirectional reflectance distribution function measurements with out -of-plane and polarimetry capabilities," (to be published).

[15] R. M. A. Azzam, "Photopolarimetric measurement of the Mueller matrix by Fourier analysis of a single detected signal," Opt. Lett. **2**, 148 (1978).

[16] R. A. Chipman, "Polarimetry," in *Handbook of Optics, Vol. II*, Michael Bass, ed., pp. 22.1–22.37 (McGraw-Hill, New York, 1995).

[17] B. W. Scheer, "Development of a physical haze and microroughness standard," Proc. SPIE **2862**, 78–95 (1996).

[18] Certain commercial equipment, instruments, or materials are identified in this paper in order to specify the experimental procedure adequately. Such identification is not intended to imply recommendation or

endorsement by the National Institute of Standards and Technology, nor is it intended to imply that the materials or equipment identified are necessarily the best available for the purpose.

[19] C. Asmail, J. Fuller, and R. Parks, "Status of Bidirectional Reflectance Distribution Function (BRDF) Calibration Standards Development," Proc. SPIE **1993**, 44–53 (1993).

[20] T. A. Germer, and C. C. Asmail, Provisional U.S. Patent Application filed.